Werk

Jahr: 1986
Kollektion: fid.geo
Signatur: 8 Z NAT 2148:59
Digitalisiert: Niedersächsische Staats- und Universitätsbibliothek Göttingen
Werk Id: PPN1015067948_0059
PURL: http://resolver.sub.uni-goettingen.de/purl?PPN1015067948_0059

LOG Id: LOG_0031
LOG Titel: Comparison of fault-plane solutions and moment tensors
LOG Typ: article

Übergeordnetes Werk

Werk Id: PPN1015067948
PURL: http://resolver.sub.uni-goettingen.de/purl?PPN1015067948
OPAC: http://opac.sub.uni-goettingen.de/DB=1/PPN?PPN=1015067948

Contact

Niedersächsische Staats- und Universitätsbibliothek Göttingen
Georg-August-Universität Göttingen
Platz der Göttinger Sieben 1
37073 Göttingen
Germany
Email: gdz@sub.uni-goettingen.de

J Geophys (1986) 59:112–118

Journal of Geophysics

Comparison of fault-plane solutions and moment tensors

Klaus-G. Hinzen
Bundesanstalt für Geowissenschaften und Rohstoffe, Stilleweg 2, D-3000 Hannover 51, Federal Republic of Germany

Abstract. In the last three or four years moment tensors have been obtained for most earthquake sources with seismic moments $M_0 > 10^{24}$ dyne · cm. Fault-plane solutions are published by NEIS for earthquakes with $M_b > 6.0$. In some cases the orientation of the best-fitting double couple of the moment tensor differs from that of the fault-plane solution. Using Euklid's norm of a matrix, the differences of the two source orientations are quantified as a distance parameter D.

120 earthquakes (January 1981–March 1983) are selected for a systematic study comparing the best-fitting double couple from the moment tensor inversion and the ordinary fault-plane solution. The assumption that the differences in source orientation increase with an increase of the non-double-couple contribution to the source is not valid for the 120 events. 11.5% of the events have small deviations from the double couple and large differences between the orientations from fault-plane solutions and moment tensors, while the 2.5% of the events with large deviations from the double couple show small differences in the source orientations derived by the two methods. None of the events has large deviations from the double couple and large differences between the orientations. Results are discussed with respect to source properties.

Key words: Moment tensor – Fault-plane solution – Non-double-couple contribution

Introduction

For more than two decades the fault-plane solution based on first P-wave motions has been the most important technique to derive focal mechanisms of earthquakes. The double-couple model, a principal requirement for this technique, proved to be acceptable for most of the observations. Hundreds of earthquake mechanisms have been studied in this way (e.g. Anderson et al., 1974; Banghar and Sykes, 1969; Forsyth, 1972; Ichikawa, 1971; Isacks et al., 1969, 1981; Johnson and Molnar, 1972; Katsumara and Sykes, 1969; Molnar, 1973; Molnar and Sykes, 1969; Ritsema, 1964, 1965, 1966; Stauder, 1968, 1975; Stauder and Bollinger, 1966; Sykes, 1967). These investigations supplied fundamental arguments for the new global tectonic model.

In the early 1970s more general formulations of seismic source mechanisms were obtained. Gilbert (1970) introduced the concept of the moment tensor, which depends on strength and orientation of the seismic source. It contains all information about the seismic source which can be obtained from far-field observations (Aki and Richards, 1980). Gilbert (1970) demonstrated the linear relation between moment tensors and seismograms. If the transfer function of the elastic medium is known, it is possible to invert source parameters from seismograms. Gilbert and Dziewonski (1975) were the first to calculate moment tensors of two deep South American earthquakes. In the following years the technique of inversion itself became the main point of interest. Mendiguren (1976), McCowman (1976), Aki and Patton (1978) and Kanamori and Given (1981) used surface-wave data: the technique was applied to body waves by Ward (1980), Strelitz (1980) and Langston (1981).

Routine determinations of moment tensors (Sipkin, 1982) and Centroid-Moment Tensors (CMT) (Dziewonski et al., 1981) were the first steps to utilize the advantages of inversion techniques for the study of global tectonics. The work of Dziewonski and Woodhouse (1983), Giardini and Woodhouse (1984) and Giardini (1983) proved the applicability of the CMT concept in order to study seismic sources.

However, the question arises as to what the relations between results of the inversion techniques and fault-plane solutions are and whether the differences between both kinds of source description can be interpreted. An answer to this question may help to elucidate the rupture process of special events and to find out whether the moment tensor concept can fully replace the fault-plane solution technique. The purpose of this study is a systematic comparison between published CMTs and fault-plane solutions for the time interval January 1981–March 1983.

Differences in source orientations

In a number of recent publications, moment tensors and fault-plane solutions of special events have been compared. Dziewonski and Woodhouse (1983) calculated the CMT of 201 earthquakes in 1981. One of the earthquakes discussed in detail was the event of May 25, 1981, off the west coast of the South Island of New Zealand with the seismic moment $M_0 = 2.7 \times 10^{25}$ dyne cm. The fault-plane solution, on the basis of first P-wave motions, is reported by NEIS as a reverse fault. The best-fitting double couple of the CMT is of strike-slip type. If the N31°E-striking and 66°SE-dipping plane of the CMT solution is assumed to be the fault plane, the right-lateral motion agrees well with the expected relative motion between the Pacific and Indian plates.

Choy et al. (1983) analysed teleseismic data of the January 9, 1982, New Brunswick event. The multichannel signal enhancement method and the multichannel vector deconvo-

lution method were applied. The differences for strike and slip are 14° and 21°, respectively. The dip angles of the fault planes are identical. The preferred fault-plane solution has nearly the same dip and slip angles of the fault plane compared to the results of inversion but deviates by 31° and 45° in the direction of strike.

Barker and Langston (1983) compared fault-plane solutions and moment tensors of Mammoth Lake, California, earthquakes. They found first-motion readings of teleseismic recordings to be inconsistent with mechanisms determined from local and regional *P*-wave first motions. Nevertheless, the inversion of only a few teleseismic body waves gave radiation patterns of moment tensors which are consistent with most of the first *P*-wave motions in all distances.

The validity of the double-couple model (DC), i.e. the pure shear dislocation with a constant slip direction on a plane discontinuity, is a basic requirement of the fault-plane solution technique. This precondition is not fundamental to the calculation of moment tensors. The only condition in the CMT calculation that is usually assumed is a vanishing isotropic component:

$$tr[\mathbf{M}]=0$$

where **M** is the moment tensor. The source is not constrained to be a double couple (Dziewonski et al., 1981). Therefore, the intermediate eigenvalue E_2 of the three eigenvalues E_1, E_2, E_3 does not need to equal zero, as required for the plane shear models.

The ratio of the intermediate eigenvalue E_2 and the largest eigenvalue

$$|\varepsilon|=\frac{E_2}{\mathrm{Max}(|E_1|,|E_2|)}$$

is a quantitative measure for the non-double-couple contribution to the total moment tensor. The absolute value of ε is 0 for plane shear and 0.5 for the largest possible deviation from a double couple. The latter case is interpreted by Knopoff and Randall (1970) as corresponding to a linear vector dipole or equivalently – following Gilbert (1970) – as the special case of equal minor and major double couples into which the tensor is decomposed.

Dziewonski and Woodhouse (1983) found $|\varepsilon|$-values ranging from 0 to 0.35 for shallow sources ($h\leqq 50$ km), $0\leqq|\varepsilon|\leqq 0.4$ for intermediate depth ($50\text{ km}<h\leqq 300$ km) and $0\leqq|\varepsilon|\leqq 0.3$ for deep events ($h>300$ km). The range of $|\varepsilon|$-values reveals that about 20% of the events have significant non-double-couple contributions with $|\varepsilon|>0.2$. For those earthquakes with large non-double-couple contributions, the validity of the plane shear model has to be questioned and it may be supposed that these deviations from the DC source give different orientations of the fault planes from fault-plane solutions and from the moment tensor calculation, respectively.

Distance parameter

For a systematic comparison of fault-plane solutions and moment tensors, the differences between the two source orientations must be quantified. Therefore, Euklid's norm of a matrix **A** is introduced as a measure of distance. The norm is defined as the square root of the trace of the matrix product of $\mathbf{A}^T$ and **A**, where $\mathbf{A}^T$ is the transpose of **A**:

$$||\mathbf{A}||=(tr[\mathbf{A}^T\cdot\mathbf{A}])^{1/2}.$$

The normalized matrix $\mathbf{A}_n$ is defined as:

$$\mathbf{A}_n=\frac{\mathbf{A}}{||\mathbf{A}||}.$$

The distance parameter for two solutions, which are represented by matrices **A** and **B**, containing the six independent elements of the moment tensor is:

$$D(\mathbf{A},\mathbf{B})=||\mathbf{A}_n-\mathbf{B}_n||$$

where

$$0\leqq D\leqq 2.$$

If two solutions for instance have the same strike and dip angles of the fault plane and differ by 90° in the value of the slip angle, the distance parameter is $D=1$. Reverse sense of motion, which is equivalent to a 180° difference in slip angle, results in the maximum distance parameter $D_{max}=2$. For the latter case, the directions of the principal axes *P* and *T*, corresponding to the smallest and largest eigenvalue, respectively, are exchanged.

Comparison of orientations

The Centroid-Moment Tensors of Dziewonski and Woodhouse (1983) and Dziewonski et al. (1983a, b) represent a large data base of homogeneous inversion results for worldwide seismicity. Nearly 600 CMTs of earthquakes (January 1981–March 1983) have been computed from body- and mantle-wave data of the Global Digital Seismograph Network (GDSN). For comparison, fault-plane solutions are taken from the monthly listings of NEIS. The lower magnitude bound for routine fault-plane solutions is $M_b=6.0$. Among these data, 120 earthquakes are used in this comparison. Date, origin time (NEIS), depth of the centroid source in kilometres and the scalar seismic moment in dyne·cm are listed in Table 1 together with the quantities *D* and $|\varepsilon|$.

The distance parameter *D* has been calculated between the moment tensor corresponding to the douple-couple orientation of the fault-plane solution and the moment tensor of the best-fitting double couple of the Centroid-Moment Tensor. The six independent values of the moment tensor corresponding to the fault-plane solution were determined from the angles of orientation of the source, ϕ, δ, λ (Aki and Richards, 1980), where ϕ, δ and λ are strike, dip and slip angle, respectively. Figure 1 shows the relation between *D* and $|\varepsilon|$, where $|\varepsilon|$ is calculated from CMT eigenvalues.

Only four events have distance parameters $D>1.0$. These are indicated by small arrows identified with the event number. The *P*- and *T*-axes of events Nos. 3 and 4 (both January 23, 1981) are exchanged with respect to those of the moment tensor: the distance parameters reach nearly the maximum value ($D>1.9$). By a classification of $|\varepsilon|$ and *D* values, Fig. 1 is divided into six ranges denoted by *i–vi*. The non-double-couple contribution is divided into three classes:

low $\|\varepsilon\|$:	$0.0\leqq\|\varepsilon\|<0.17$
intermediate $\|\varepsilon\|$:	$0.17\leqq\|\varepsilon\|<0.33$
high $\|\varepsilon\|$:	$0.33\leqq\|\varepsilon\|$

and the distance parameter is divided into two classes:

low *D*:	$0.0\leqq D<0.5$
high *D*:	$0.5\geqq D.$

Table 1. Distance parameters D between the fault-plane solution (NEIS) and the best double couple of Centroid Moment Tensors (Dziewonski et al., 1981) are listed for 120 earthquakes from January 1981 to March 1983. In addition, the non-double-couple contribution of the CMT, depth and seismic moment are given

No.	Date	Time (h min s)	h (km)	M_0 (dyne·cm)	exp	D	$\lvert\varepsilon\rvert$	Region
1	18 01 81	18 17 24	20	3.69	26	0.07	0.06	Honshu
2	19 01 81	15 11 01	10	1.17	26	0.48	0.19	Iran
3	23 01 81	21 13 51	15	0.99	26	1.94	0.01	Sichuan
4	23 01 81	21 54 42	10	2.98	26	1.92	0.14	Atl. Indian Ridge
5	24 02 81	20 53 38	20	1.29	26	0.08	0.04	Greece
6	04 03 81	21 58 06	29	3.48	25	0.10	0.24	Greece
7	06 03 81	19 42 59	24	1.18	26	0.62	0.02	Central Am.
8	24 04 81	21 50 06	44	2.25	26	0.13	0.04	Vanuatu Island
9	27 04 81	18 17 34	10	7.53	25	0.08	0.07	Maquarie Island
10	25 05 81	05 25 14	20	2.70	27	0.46	0.10	South Island N.Z.
11	03 06 81	05 42 44	10	8.07	25	0.07	0.06	South Atlantic Ridge
12	06 07 81	03 08 24	58	2.59	27	0.29	0.25	Loyalty Island
13	07 07 81	21 10 57	10	2.46	26	0.29	0.02	Mid Atlantic Ridge
14	15 07 81	07 59 08	30	5.76	26	0.15	0.04	Vanuatu
15	28 07 81	17 22 24	20	6.68	26	0.95	0.21	Iran
16	01 09 81	09 29 31	20	1.94	27	0.64	0.06	Samoa Island
17	03 09 81	05 35 44	36	7.54	25	0.56	0.01	Kuril Island
18	17 09 81	08 23 24	30	1.64	26	0.17	0.14	Loyalty Island
19	16 10 81	03 25 42	40	5.11	26	0.33	0.09	Chile
20	25 10 81	03 22 15	32	7.00	26	0.00	0.07	Mexico
21	03 11 81	13 47 34	10	5.15	25	0.14	0.00	Oregon
22	06 11 81	16 47 49	15	0.91	26	0.52	0.20	Papua
23	07 11 81	03 29 51	66	3.26	26	0.32	0.21	Chile
24	22 11 81	15 05 20	29	5.27	25	0.02	0.03	Cuzon
25	12 12 81	04 52 37	15	4.49	25	0.58	0.03	Ryukyu Island
26	19 12 81	14 10 50	22	2.41	26	0.00	0.06	Aegean Sea
27	24 12 81	04 33 20	19	2.11	26	0.05	0.02	Kermadec
28	26 12 81	17 05 32	30	4.57	26	0.01	0.08	Kermadec
29	27 12 81	17 39 13	22	3.34	25	0.07	0.12	Aegean Sea
30	01 01 82	18 51 01	37	9.00	25	0.17	0.02	Bonin Island
31	03 01 82	14 09 50	10	4.76	26	0.27	0.01	Mid Atlantic Ridge
32	07 01 82	08 42 50	15	7.93	24	0.90	0.25	Gilbert Island
33	09 01 82	12 53 51	10	1.94	24	0.99	0.18	Brunswick
34	11 01 82	06 10 06	17	4.96	26	0.02	0.01	Philippine Island
35	18 01 82	19 27 24	9	9.38	25	0.13	0.10	Aegean Sea
36	24 01 82	06 08 56	19	1.05	26	0.05	0.04	Philippine Island
37	20 02 82	13 26 50	10	1.92	26	1.00	0.20	Santa Cruz
38	20 02 82	19 18 20	30	6.06	25	0.25	0.38	Honshu
39	11 03 82	10 32 27	36	7.43	25	0.47	0.27	Sumbawa Island
40	21 03 82	02 32 07	37	2.64	26	0.58	0.07	Hokaido
41	06 04 82	19 56 53	43	1.44	26	0.13	0.14	Mexico
42	02 05 82	11 19 38	20	4.52	25	0.02	0.00	Kermadec
43	31 05 82	10 21 15	19	7.15	25	0.10	0.06	Komandorsky
44	31 05 82	15 18 55	23	5.86	25	0.03	0.02	W. Caroline Island
45	02 06 82	12 37 34	11	3.95	25	0.95	0.07	Tonga
46	07 06 82	06 52 37	11	2.90	26	0.21	0.01	Mexico
47	07 06 82	10 59 40	19	2.66	26	0.17	0.01	Mexico
48	19 06 82	06 21 58	52	1.05	27	0.47	0.07	El Salvador
49	22 06 82	04 18 40	473	1.77	27	0.05	0.07	Banda Sea
50	30 06 82	01 57 34	21	4.45	26	0.16	0.12	Kuril Island
51	04 07 82	01 20 06	552	1.25	26	0.20	0.17	Ryukyu Island
52	07 07 82	10 43 03	10	4.60	26	0.06	0.25	Maquarie Island
53	23 07 82	14 23 53	27	3.92	26	0.03	0.00	Honshu
54	03 08 82	06 04 39	17	6.15	24	0.11	0.16	Mariana
55	05 08 82	20 32 52	24	3.20	26	0.01	0.02	Santa Cruz
56	07 08 82	20 56 22	18	5.57	25	0.21	0.15	Bali
57	12 08 82	02 13 08	33	6.02	25	0.08	0.06	New Ireland
58	14 08 82	14 27 40	114	1.40	25	0.33	0.08	Papua
59	17 08 82	22 22 24	23	3.98	25	0.17	0.04	Mediterranean Sea
60	19 08 82	15 59 01	25	1.19	26	0.32	0.04	Panama
61	22 08 82	03 42 36	56	3.05	24	0.07	0.02	Vanuatu Island
62	23 08 82	16 40 19	10	2.25	24	0.57	0.16	Honshu
63	26 08 82	05 22 59	92	1.13	25	0.01	0.03	Equador
64	03 09 82	01 32 00	10	1.56	25	0.00	0.05	Kuril Island

Table 1 (continued)

No.	Date	Time (h min s)	h (km)	M_0 exp (dyne·cm)		D	$\|\varepsilon\|$	Region
65	03 09 82	23 39 39	10	5.50	25	0.07	0.09	Tonga
66	04 09 82	13 31 14	10	1.45	25	0.04	0.09	Fiji Island
67	06 09 82	01 47 02	156	2.02	26	0.54	0.20	Honshu
68	15 09 82	20 22 55	167	3.28	25	0.60	0.24	Peru
69	17 09 82	13 28 24	561	1.73	25	0.09	0.05	Fiji Island
70	28 09 82	15 14 36	42	4.93	25	1.22	0.27	Fiji Island
71	05 10 82	09 14 32	10	8.71	24	0.56	0.12	Vanuatu Island
72	05 10 82	21 39 12	10	2.78	24	0.97	0.06	South Atlantic Ridge
73	07 10 82	07 15 56	521	1.33	26	0.09	0.06	Banda Sea
74	11 11 82	00 43 45	29	2.59	25	0.09	0.30	Sumatera
75	14 11 82	08 29 20	110	2.60	24	0.02	0.00	Kamchatka
76	16 11 82	17 25 53	10	1.45	25	0.34	0.10	Vanuatu Island
77	18 11 82	14 57 52	190	8.19	25	0.25	0.04	Ecuador
78	19 11 82	04 27 13	10	1.06	26	0.28	0.01	Peru
79	03 12 82	22 29 59	229	6.13	25	0.24	0.04	Vanuatu Island
80	05 12 82	05 48 25	65	4.02	24	0.29	0.18	Solomon Island
81	13 12 82	09 12 48	10	2.52	25	0.32	0.10	W. Arab. Penin.
82	16 12 82	00 40 48	33	6.11	25	0.25	0.06	Hindukush
83	17 12 82	02 43 03	94	6.34	25	0.11	0.05	Taiwan
84	19 12 82	17 43 54	29	1.98	27	0.16	0.06	Tonga Island
85	20 12 82	02 58 10	10	3.28	25	0.19	0.12	Tonga Island
86	28 12 82	06 37 42	22	2.09	25	0.01	0.10	Honshu
87	28 12 82	13 49 29	25	1.57	25	0.06	0.03	Philippine Island
88	01 01 83	05 31 56	172	3.16	25	0.08	0.00	Peru
89	08 01 83	11 21 29	53	3.00	25	0.13	0.08	Tonga
90	10 01 83	12 32 21	565	4.78	24	0.13	0.24	Sant. Estero
91	16 01 83	22 10 12	230	8.26	25	0.04	0.04	Papua
92	17 01 83	12 41 29	10	2.35	26	0.06	0.15	Greece
93	18 01 83	15 23 36	28	5.08	25	0.72	0.24	Sandwich Island
94	24 01 83	08 17 39	36	2.06	26	0.52	0.14	Mexico
95	24 01 83	16 34 08	32	8.52	24	0.44	0.24	N. Atlantic Ocean
96	24 01 83	23 09 21	73	1.71	26	0.23	0.42	Andaman Island
97	26 01 83	16 02 21	224	3.66	26	0.14	0.39	Kermadec
98	31 01 83	21 17 31	10	1.89	24	1.16	0.03	Gilbert Island
99	07 02 83	18 23 17	52	1.62	25	0.08	0.05	Kermadec
100	12 02 83	08 47 13	23	3.19	25	0.17	0.12	Philippine Island
101	14 02 83	00 23 19	35	1.30	25	0.03	0.13	Caroline Island
102	14 02 83	03 20 04	19	7.12	25	0.04	0.07	Alaska
103	14 02 83	08 10 04	40	1.00	25	0.11	0.16	Alaska
104	19 02 83	20 14 23	566	1.11	25	0.10	0.30	Philippine Island
105	20 02 83	10 49 54	39	3.71	25	0.12	0.12	Philippine Island
106	25 02 83	22 03 56	217	3.56	24	0.03	0.06	Papua
107	26 02 83	07 10 59	45	3.62	25	0.04	0.01	Kuril Island
108	27 02 83	12 14 21	73	1.52	25	0.04	0.06	Honshu
109	28 02 83	05 44 24	28	1.52	25	0.02	0.14	Kuril Island
110	08 03 83	17 06 37	85	8.38	24	0.01	0.05	Windward Island
111	10 03 83	00 27 48	37	1.23	25	0.02	0.12	Kuril Island
112	11 03 83	03 10 42	58	4.83	24	0.22	0.10	Papua
113	12 03 83	00 53 40	11	1.51	25	0.03	0.23	Banda Sea
114	12 03 83	01 36 36	16	9.25	25	0.32	0.09	Banda Sea
115	15 03 83	19 58 30	21	6.58	25	0.06	0.10	Philippine Island
116	18 03 83	09 05 50	70	4.63	27	0.13	0.11	New Ireland
117	20 03 83	13 45 49	65	4.13	25	0.50	0.08	New Ireland
118	21 03 83	07 44 18	52	1.18	26	0.01	0.05	Tonga
119	23 03 83	06 09 29	49	4.46	25	0.05	0.18	Solomon Island
120	23 03 83	23 51 07	33	2.23	25	0.10	0.14	Greece

The percentages of events in the ranges are:

range *i*	(low D,	low $\|\varepsilon\|$)	66.6%
range *ii*	(low *D*,	intermediate $\|\varepsilon\|$)	11.5%
range *iii*	(low *D*,	high $\|\varepsilon\|$)	2.5%
range *iv*	(high *D*,	low $\|\varepsilon\|$)	11.5%
range *v*	(high *D*,	intermediate $\|\varepsilon\|$)	7.4%
range *vi*	(high *D*,	high $\|\varepsilon\|$)	0.0%.

78% of the events (range *i* and *iv*) are well explained by the double-couple model, while 2.5% show large non-double-couple contributions. Intermediate $|\varepsilon|$-values are found for 19% (range *ii* and *v*). 11.5% (range *iv*) of the events show large differences in the source orientations derived by the two methods, though the non-double-couple contributions is small. A striking feature of Fig. 1 is the emptyness

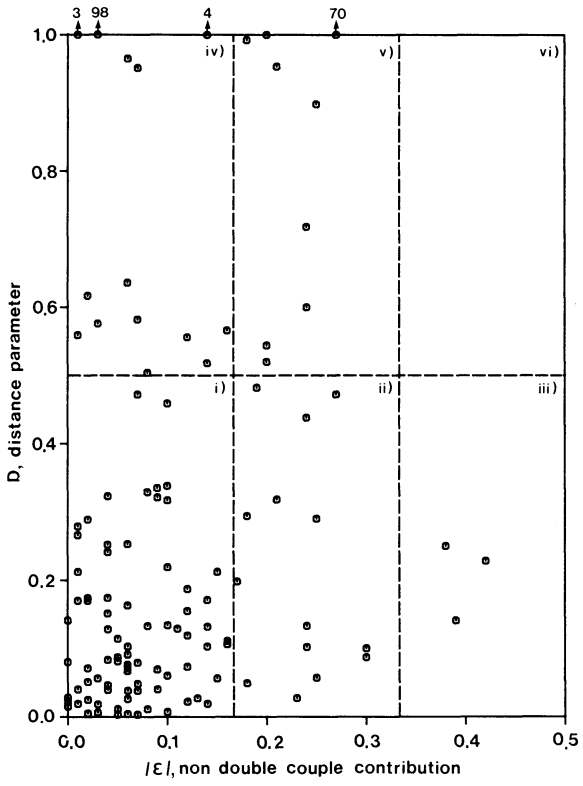

Fig. 1. The distance parameters between fault-plane solutions, FPS (NEIS), and the best-fitting double couple of Centroid Moment Tensors, CMT (Dziewonski et al., 1981), of 120 earthquakes are shown as a function of the non-double-couple contribution of the CMTs. The *arrows at the top* indicate those events with $D > 1.0$. The numbers are those of Table 1

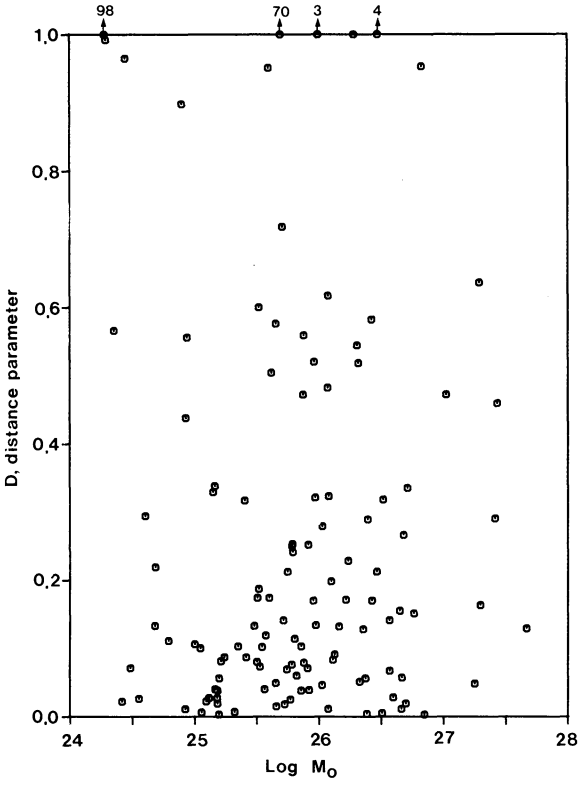

Fig. 2. The distance parameters between fault-plane solutions and the best-fitting double couple of Centroid Moment Tensors are plotted as a function of the logarithm of the scalar seismic moment. M_0 is taken in dyne cm. The notation is the same as in Fig. 1

of range *vi*, i.e. no event with large $|\varepsilon|$ and large D is found among the 120 earthquakes. Nevertheless, 2.5% have small distance parameters and large non-double-couple contributions (range *iii*). In Figs. 2 and 3 the distance parameters are plotted versus the logarithm of the scalar seismic moment, M_0 in dyne · cm, and versus depth of the centroid. The large scatter of distance parameters in the four orders of magnitude of M_0 give no indication for any dependence of D on the strength of the earthquake. From Fig. 3 it may be suggested that the averaged values of D decrease with increasing depth. This speculation can only be verified after more data of intermediate and deep earthquakes are incorporated.

Discussion and conclusions

The fault-plane solution technique and the Centroid-Moment Tensor determination use different spatio-temporal dimensions of the seismic source. The fault-plane solution technique uses the direction of the very first P-wave motion from the vertical component. The first-motion readings contain only information about the situation at rupture initiation, whereas the inversion of entire waveform for the optimum point source, like the Centroid-Moment Tensor, is an average over the whole spatio-temporal dimension of the source. If, for example, the earthquake is divided into two or more successive subevents, the ordinary fault-plane solution will only represent the orientation of the first subevent. The moment tensor is a mean solution for all events if the inversion process is not constrained to form two or more events. Therefore, in a seismotectonic interpretation of source orientations, the influence of the method used must be kept in mind.

The 19% of events in ranges *iv* and *v* show that large distance parameters exist in spite of small or intermediate non-double-couple contributions. This may be an indication for a change of fault-plane geometry or slip direction after the initiation of rupture. The 11.5% in range *iv* show that the large distance parameters can not be attributed to the deviation from the plane shear mechanism. The events Nos. 38, 96 and 97 in range *iii* represent the case that the orientation of the fault-plane solution fits quite well with the orientation derived from the moment tensor, though the large $|\varepsilon|$-value indicates striking differences to the simple plane shear model. If the large $|\varepsilon|$-values are no effect of the procedure, for example due to lateral-inhomogenities in the source region, a multiple rupture process on one or more focal planes with stable orientation may cause this effect.

Although the inversion of moment tensors is a very powerful and objective tool in the determination of source parameters, it cannot replace the fault-plane solution completely. In the case of a complicated and multiple rupture process, fault-plane solution and, in addition, master event techniques and forward modelling of waveforms (Bruestle, 1985) have to be applied for a detailed analysis of the source mechanism.

The distance parameter D proved to be a good measure

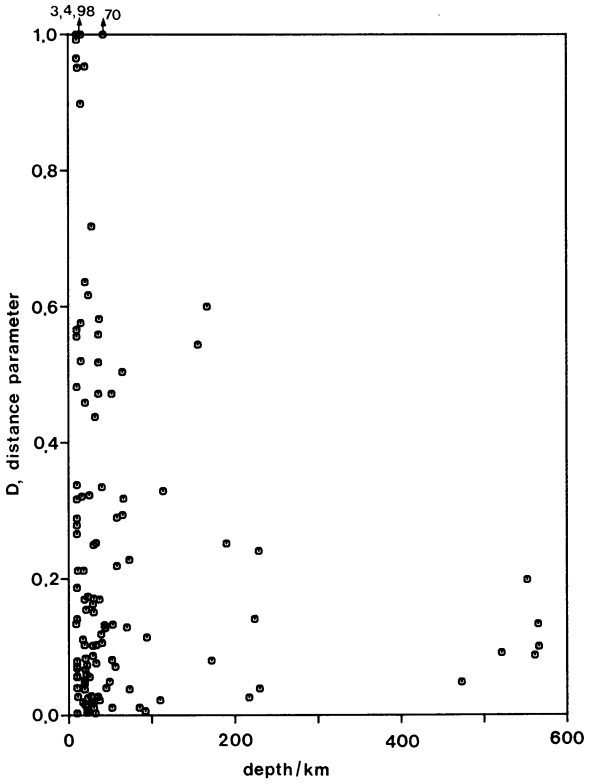

Fig. 3. The distance parameters between fault-plane solutions and the best double couple of Centroid Moment Tensors are shown as a function of source depth. The depth is that of the centroid. The notation is the same as in Fig. 1

for a comparison of source orientations of earthquakes obtained by different methods. In this study results of two methods applied to one earthquake have been examined. The distance parameter may also be used for other purposes. For example, applied to a cluster analysis it can help to discriminate between earthquake mechanisms of different types and to test whether an event belongs to a certain group of source mechanisms or not.

Acknowledgements. The basic work for this study was carried out during my time at the Institut für Geophysik of the Ruhr-Universität Bochum. I am grateful to R.-G. Ferber and H.P. Harjes with whom I had helpful discussions over the course of this research. I thank two reviewers for their comments and H.-U. Worm for carefully reading the manuscript.

References

Aki, K., Patton, H.: Determination of seismic moment tensor using surface waves. Tectonophys. **49**, 213–222, 1978

Aki, K., Richards, P.G.: Quantitative seismology, Vol. 1, 557 pp. San Francisco: Freeman 1980

Anderson, R.N. Forsyth, D.W., Molnar, P., Mammerickx, J.: Fault plane solutions of earthquakes on the Nazca plate boundaries and the Easter plate. Earth Planet. Sci. Lett. **24**, 188–202, 1974

Banghar, A.R., Sykes, L.R.: Focal mechanisms in the Indian Ocean and adjacent regions, J. Geophy. Res. **74**, 632–649, 1969

Barker, J.S., Langston, C.A.: A teleseismic body-wave analysis of the May 1980 Mammoth Lakes, California, earthquakes Bull. Seism. Soc. Am. **73**, 419–434, 1983

Bruestle, W.: Der Bruchvorgang im Erdbebenherd – Untersuchung ausgewählter Erdbeben mit beobachteten und synthetischen Seismogrammen. Ber. d. Inst. f. Met. u. Geoph. Univ. Frankfurt, Nr. 63, 1985

Choy, G.L., Boatwright, J., Dewey, J.W., Sipkin, S.A.: A teleseismic analysis of the New Brunswick earthquake of January 9, 1982. J. Geophys. Res. **88**, 2199–2212, 1983

Dziewonski, A.M., Chou, T.-A., Woodhouse, J.H.: Determination of earthquake source parameters from waveform data for studies of global and regional seismicity. J. Geophys. Res. **86**, 2825–2852, 1981

Dziewonski, A.M., Friedman, A., Giardini, D., Woodhouse, J.H.: Global seismicity of 1982: Centroid-Moment Tensor Solutions for 308 earthquakes. Phys. Earth Planet. Inter. **33**, 76–90, 1983a

Dziewonski, A.M., Friedman, A., Woodhouse, J.H.: Centroid-Moment Tensor Solutions for January-March, 1983. Phys. Earth Planet. Inter. **33**, 71–75, 1983b

Dziewonski, A.M., Woodhouse, J.H.: An experiment in systematic study of global seismicity: Centroid-Moment Tensor Solutions for 201 moderate and large earthquakes of 1981. J. Geophys. Res. **88**, 3247–3271, 1983

Forsyth, D.W.: Mechanisms of earthquakes and plate motions in the East Pacific. Earth Planet. Sci. Lett. **17**, 189–193, 1972

Giardini, D.: Systematic analysis of deep seismicity: 200 Centroid-Moment Tensor solutions for earthquakes between 1977 and 1980. Geophys. J. R. Astron. Soc. **77**, 883–914, 1983

Giardini, D., Woodhouse, J.H.: Deep seismicity and modes of deformation in the Tonga subduction zone. Nature **307**, 505–509, 1984

Gilbert, F.: Exicitation of normal modes of the earth by earthquake sources. Geophys. J. R. Astron. Soc. **22**, 223–226, 1970

Gilbert, F., Dziewonski, A.M.: An application of normal mode theory to the retrieval of structural parameters and source mechanisms from seismic spectra. Phil. Trans. Roy. London. Ser. A, **278**, 187–269, 1975

Ichikawa, M.: Reanalysis of mechanism of earthquakes which occurred in and near Japan, and statistical studies of the nodal plane solutions obtained, 1926–1968. Geophys. Mag. JMA, **35**, 207–274, 1971

Isacks, B., Cardwell, K.R., Chatelain, J.-L., Barazangi, M., Martelot, J.-M., Chinn, D., Louat, R.: Seismicity and tectonics of the central New Hebrides island arc. In: Earthquake Prediction, D.W. Simpson and P.G. Richards, eds. Washington: Am. Geophys. Union 1981

Isacks, B., Sykes, L.R., Oliver, J.: Focal mechanisms of deep and shallow earthquakes in the Tonga-Kermadeo Region and tectonics of island arcs. Bull. Geol. Soc. Am. **80**, 1443–1470, 1969

Johnson, T., Molnar, P.: Focal mechanisms of southwest Pacific. J. Geophys. Res. **77**, 5000–5032, 1972

Kanamori, H., Given, J.W.: Use of long-period surface waves for fast determination of earthquake source parameters. Phys. Earth Planet Inter. **27**, 8–31, 1981

Katsumata, M., Sykes, L.R.: Seismicity and tectonics of the western Pacific: Izu-Mariana-Caroline and Ryukyu-Taiwan Regions. Bull. Geol. Soc. Am. **74**, 5923–5948, 1969

Knopoff, L., Randall, M.J.: The compensated linear vector dipole: a possible mechanism for earthquakes. J. Geophys. Res. **75**, 4957–4963, 1970

Langston, C.A.: Source inversion of seismic waveforms: the Koyna, India earthquake of 13 September 1967. Bull. Seism. Soc. Am. **71**, 1–24, 1981

McCowman, D.W.: Moment tensor representation of surface waves. Geophys. J. R. Astron. Soc. **44**, 595–599, 1976

Mendiguren, J.: Inversion of surface wave data in source mechanism studies. J. Geophys. Res. **82**, 889–894, 1976

Molnar, P.: Fault plane solutions of earthquakes and directions of motion in the Gulf of California Ribera fracture zone. Geol. Soc. Amer. Bull. **84**, 1651–1658, 1973

Molnar, P., Sykes, L.R.: Tectonics of the Caribbean and Middle American Regions from focal mechanism and seismicity studies. Bull. Geol. Soc Am. **88**, 1639–1684, 1969

Ritsema, A.R.: Some reliable fault plane solutions. Pure Appl. Geophys. **59**, 58–74, 1964
Ritsema, A.R.: The mechanisms of some deep and intermediate earthquakes in the region of Japan. Bull. Tokyo Univ. Earthq. Res. Inst. **43**, 39–52, 1965
Ritsema, A.R.: The fault plane solutions of earthquakes of Athe Hindu Kush centre. Tectonophys. **3**, 147–163, 1966
Sipkin, S.A.: Estimation of earthquake source parameters by inversion of waveform data: synthetic waveforms. Phys. Earth Planet. Inter. **30**, 242–259, 1982
Stauder, W.: Mechanism of the Rat Island earthquake sequence of February 4, 1965 with relation to island arcs and seafloor spreading. J. Geophys. Res. **73**, 3847–3858, 1968
Stauder, W.: Subduction of the Nazca plate under Peru as evidenced by focal mechanisms and by seismicity. J. Geophys. Res. **80**, 1053–1064, 1975
Stauder, W., Bollinger, G.A.: The focal mechanism of the Alaska earthquake of March 28., 1964 and its aftershock sequence. J. Geophys. Res. **71**, 5283–529, 1966
Strelitz, R.A.: The fate of the downgoing stab: study of the moment tensor from body waves of complex deep-focus earthquakes. Phys. Earth Planet. Inter. **21**, 83–96, 1980
Sykes, L.R.: Mechanism of earthquakes and nature of faulting on the mid-oceanic ridges. J. Geophys. Res. **72**, 2131ff, 1967
Ward, S.N.: Body wave calculations using moment tensor sources in spherically symmetric, inhomogenious media. Geophys. J. R. Astron. Soc. **60**, 53–66, 1980

Received July 11, 1985; revised version December 16, 1985
Accepted December 18, 1985